



Journal homepage:
<http://www.bsu.edu.eg/bsujournals/JVMR.aspx>

Online ISSN: 2357-0520

Print ISSN: 2357-0512



Original Research Article

Normal Cross-sectional Anatomy and Magnetic Resonance Imaging of Pastern and Coffin Joints in Camel

Ibrahim, A.H.*, Adam, Z.E. and Mohamed G. Tawfik

Anatomy and Embryology Department, Faculty of Veterinary Medicine, Beni-Suef University, Beni-Suef 62511, Egypt

ABSTRACT

The present study aimed to describe the normal cross-sectional anatomy and magnetic resonance imaging of the pastern and coffin joints of the dromedary camel. This study was conducted on twelve distal limbs (fore and hind limbs) of fresh cadavers from three healthy adult camels. The specimens were normal with no orthopedic disorders. Twelve distal limbs were scanned using a 1 Tesla MRI scanner and then injected with colored latex to be sectioned into sagittal, dorsal, and transverse slices. Cross anatomical sections were matched with their corresponding MR images for identification and evaluation of the clinically relevant anatomical structures that appeared with different signal intensities on MRI scans. The present study revealed that all the soft tissues of the pastern and coffin joints of the dromedary camels were clearly depicted on the obtained MR images. However, the palmar/plantar ligaments of the pastern joint and ligaments of the navicular cartilage could not be identified on the MR images. The annotated anatomical sections with their corresponding MR images could be used as a normal anatomical reference for the interpretation of some clinical diseases in the pastern and coffin joints of the dromedary camel.

ARTICLE INFO

Received: 29/04/ 2019

Accepted: 30/07/2019

Published online: 02/08/2019

Keywords:

Anatomy, Coffin joint, Camel, Magnetic resonance imaging, Pastern joint

*Corresponding author: Ibrahim, A.H. Anatomy and Embryology Department, Faculty of Veterinary Medicine, Beni-Suef University, Beni-Suef 62511, Egypt. E-mail address: d.azzamohamed88@gmail.com

1. Introduction

Camel population is found in Egypt, Saudi Arabia, Iraq, Sudan, Iran, Somaliland, India, China and many other countries (Monfared 2013). Camel is capable to overcome the harsh climate of the desert and able to survive and produce under the difficult environmental conditions (Sadegh et al. 2007). In developing countries, it is used as an essential source of milk, meat and hide (Ahmad et al. 2010). Lameness is a critical problem due to its adverse economic impact on the dairy animals (Solano et al. 2015). In addition, lameness in camels appears with a different pattern compared to the bovine and equine, due to the particular anatomy of camel limbs (Al-Juboori 2013). These conditions require awareness of the normal gross anatomical structure and improvement of high definitive diagnostic imaging techniques for clarification and evaluation of the orthopedic affections.

There is a growing awareness in the use of the magnetic resonance imaging (MRI) and computed tomography (CT) as high definitive diagnostic imaging techniques in veterinary practices (Nuss et al. 2011). However, limited accessibility, need for animal general anesthesia and high costs diminish the valuable using of these diagnostic modalities in the veterinary practice (Arencibia et al. 2000). Nevertheless, improvement in availability of these imaging tools increases the requirement of their use in animal medicine (Pollard and Puchalski 2011). Even though many MRI studies had been done on the animal digits (El-Nahas et al. 2015 in camel; Abdellatif et al. 2018 in bovine; Sampson and Tucker 2007 in horse). However, more details on the cross sectional anatomy in corresponding to the MR imaging are still needed on the pastern and coffin joints of the dromedary camels. Hence, the current study aimed to provide a detailed anatomic reference on the cross sectional anatomy and MR imaging of the pastern and coffin joints in dromedary camels to assist as a helpful database reference for evaluation of the clinical disorders in these joints.

2. Materials and methods

2.1. Animals

This study was conducted on twelve (n=12) distal limbs (fore and hind) from fresh cadavers of three

adult healthy dromedary camels (Average age 2-4 years and average weight about 350-500 kg.). The limbs were obtained from the local slaughterhouse at Beni-Suef Governorate. The specimens were grossly examined and were apparently normal with no musculoskeletal disorders.

2.2. Magnetic resonance imaging

MRI examination was achieved on the twelve distal limbs (6 forelimbs and 6 hind limbs) of fresh cadavers. The imaging was performed within three hours after slaughtering. Limbs were located with their palmar / plantar aspects as the dependent portion and their long axis perpendicular to the examination table. T1-weighted MR images (TR = 1900 ms, TE = 2.74 ms, slice thickness = 2mm) were obtained in sagittal, dorsal and transverse planes using a 1 Tesla MR scanner (Philips Medical system Intera, 1T MRI; Philips GmbH, Hamburg, Germany).

2.3. Preparation of the anatomical cross sections

The scanned limbs were injected with colored latex. The needle was introduced into the dorsal pouches of the pastern and coffin joints just abaxial to the tendinous parts of the digital extensor tendons. The limbs were frozen at -18°C for one week. Then the frozen specimens were sectioned into sagittal (forelimbs=2, hind limbs=2), dorsal (forelimbs=2, hind limbs=2) and transverse (forelimbs=2, hind limbs=2) slices starting at the middle of the first phalanx till the coffin joint in 1cm slice thickness using an electric band saw. Tap water was used for gentle cleaning of the anatomic sections to be photographed. The anatomical sections were grossly inspected, determined and selected in correlation to their corresponding MR images.

2.4. Comparison of the cross anatomical sections and the obtained MR images

Cross sections of the pastern and coffin joints were compared to their corresponding MR images. For evaluation of the anatomical structures of the pastern and coffin joints, six MR images were selected in correspondence to the anatomical structures of the gross sections from the same specimens, one in a sagittal plane (Fig. 1), one in a dorsal plane (Fig. 2) and four in transverse planes (Figs. 3-6).

3. Results

The cross anatomical sections and magnetic resonance images (MRI) gave a precise reference for interpretation of the MRI of pastern and coffin joints in dromedary camel. Articular cartilages of the second and third phalanges were clearly differentiated from the bony structures as a thin plate of high signal intensity (**Figs. 1, 2**). Subchondral bone was visualized as a thin layer of low signal intensity which could be easily recognized from articular cartilage at the extremity of each bone (**Figs. 1, 2**). Cancellous bone appeared at extremities of the second and third phalanges with a high signal intensity (**Figs. 1, 2**). Medullary cavity of the second and third phalanges appeared with a high signal intensity, while the cortical bone could be visualized with a low signal intensity (**Figs. 1, 2**).

The middle scutum and navicular cartilage were clearly defined on the sagittal MR images with high signal intensities (**Fig. 1**). Moreover, the nails had a heterogeneous high signal intensity (**Fig. 1**), while the sole of the footpad appeared as a layer of low signal intensity between the two lines of high signal intensities (**Figs. 1, 2**).

Digital cushion had a heterogeneous high signal intensity, and the surrounding tissue had an intermediate signal intensity on the sagittal and dorsal MR images (**Figs. 1, 2**). Soft tissue structures were easily visualized on the MR images with variable signal intensities.

Extensor tendons that could be identified on the MR images included; the lateral digital extensor tendons, lateral and medial limbs of the common digital extensor tendons. These tendons appeared with homogenous low signal intensities. Margins of these tendons could be defined from the surrounding fascia that had a low intermediate signal intensity. The extensors were best identified on the transverse MR

images as two small oval structures on the dorsal aspect of each digit (**Fig. 3**). Distal to the pastern joint, these tendons were constituted by one narrow strip on the dorsal aspect of each digit representing the branches of the lateral limb of the common digital extensor tendon (**Figs. 4, 5**). Moreover, the insertion of the lateral limb of the common digital extensor tendon in the dorsal ridge of the third phalanx was clearly depicted on the sagittal MR images (**Fig. 1**).

The superficial digital flexor tendon (SDFT) and the deep digital flexor tendon (DDFT) had low signal intensities surrounded by the digital tendon sheaths which appeared with a low signal intensity (**Figs. 3-6**). At the distal third of the first phalanx, SDFT appeared deep to the DDFT prior to its insertion on the proximal extremity of the second phalanx (**Fig. 3**). Palmar/plantar to the middle scutum, DDFT appeared as a semi-circular structure (**Fig. 4**), while distal to the pastern joint, this tendon became flattened (**Figs. 5, 6**). Reposition of the flexor tendons could be visualized on the sagittal MR images (**Fig. 1**). Moreover, the inserting part of the DDFT on the flexor surface of the third phalanx was separated from the underlying digital cushion by a bursa which was well-defined on the sagittal MR images with a low signal intensity (**Fig. 1**).

The joint capsules of the pastern and coffin joints had low signal intensities, while their margins were outlined as thin lines of an intermediate signal intensity on all acquired MR images (**Figs. 1-6**). Ligaments of these joints were well-delineated on the transverse and dorsal MR images with intermediate signal intensity (**Figs. 1, 2**). The ligaments that could be clearly outlined on the MR images included; the collateral ligaments of the pastern joint, as well as the interdigital, the collateral and dorsal ligaments of the coffin joint. While the palmar/plantar ligaments of the pastern joint and ligaments of the navicular cartilage could not be defined.

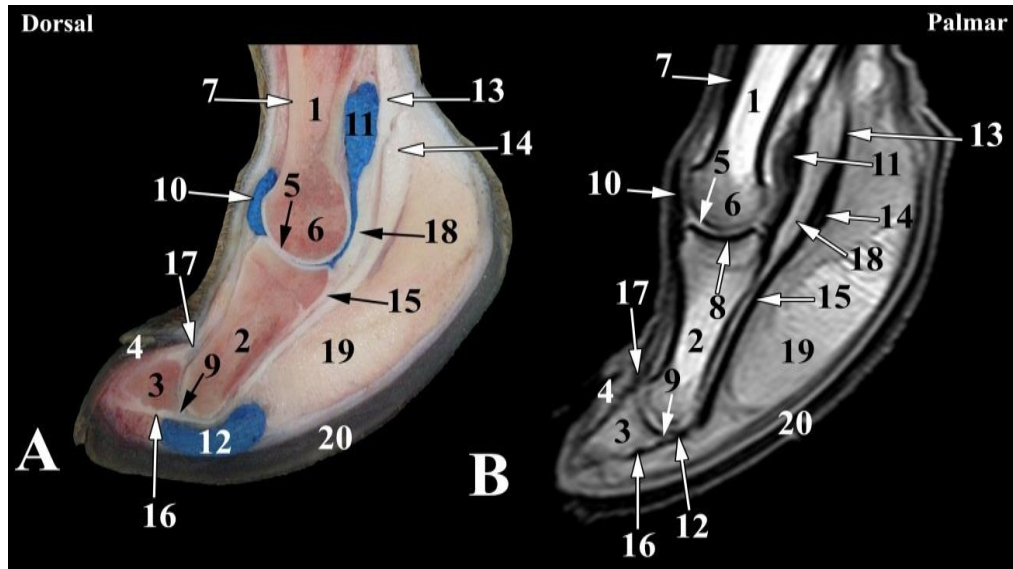


Fig. 1. Sagittal images of the right fore distal limb of the dromedary camel. **A.** Sagittal gross anatomical section; **B.** Magnetic resonance image. **1.** First phalanx; **2.** Second phalanx; **3.** Third phalanx; **4.** Nail; **5.** Articular cartilage; **6.** Cancellous bone; **7.** Cortical bone; **8.** Subchondral bone; **9.** Navicular cartilage; **10.** Dorsal synovial pouch of the pastern joint; **11.** Palmar/plantar synovial pouch of the pastern joint; **12.** Bursa between insertion of the deep digital flexor tendon and the digital cushion; **13.** Superficial digital flexor tendon; **14.** Deep digital flexor tendon; **15.** Insertion of the superficial digital flexor tendon; **16.** Insertion of the deep digital flexor tendon; **17.** Insertion of the lateral limb of the common digital extensor tendon; **18.** Middle scutum; **19.** Middle digital cushion; **20.** Sole.

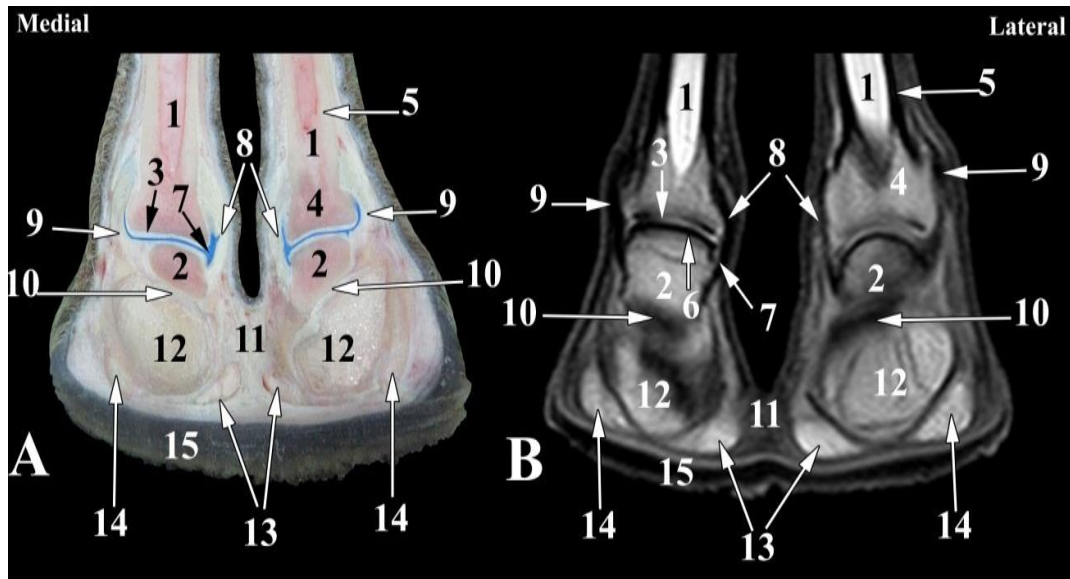


Fig. 2. Dorsal images of the pastern joint of the right forelimb of the dromedary camel at the level of the collateral ligaments attachment. **A.** Dorsal gross anatomical section; **B.** Magnetic resonance image: **1.** Proximal phalanx; **2.** Middle phalanx; **3.** Articular cartilage; **4.** Cancellous bone; **5.** Cortical bone; **6.** Subchondral bone; **7.** Joint cavity of the pastern joint; **8.** Axial collateral ligaments of the pastern joint; **9.** Abaxial collateral ligaments of the pastern joint; **10.** Deep digital flexor tendon; **11.** Interdigital ligament; **12.** Middle digital cushion; **13.** Axial digital cushion; **14.** Abaxial digital cushion; **15.** Sole.

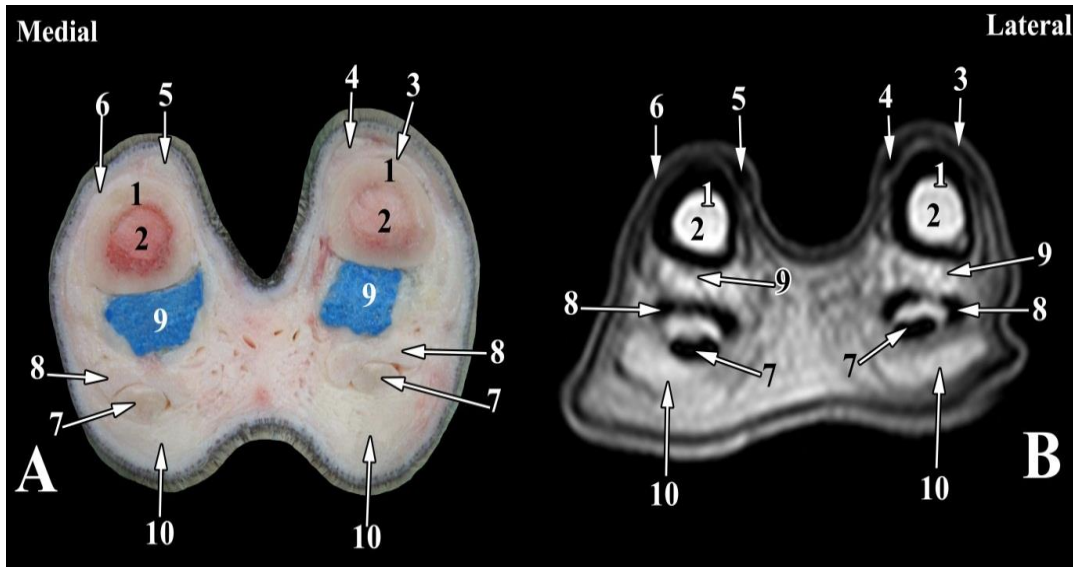


Fig. 3. Transverse images of the right fore distal limb of the dromedary camel at the level of the distal third of the proximal phalanx. **A.** Transverse gross anatomical section; **B.** Magnetic resonance image. **1.** Proximal phalanx; **2.** Medullary cavity of the proximal phalanx; **3.** Lateral digital extensor tendon; **4.** Lateral branch of the lateral limb of the common digital extensor tendon; **5.** Medial branch of the lateral limb of the common digital extensor tendon; **6.** Medial limb of the common digital extensor tendon; **7.** Deep digital flexor tendon; **8.** Superficial digital flexor tendon; **9.** Palmar synovial pouch of the pastern joint; **10.** Digital cushion.

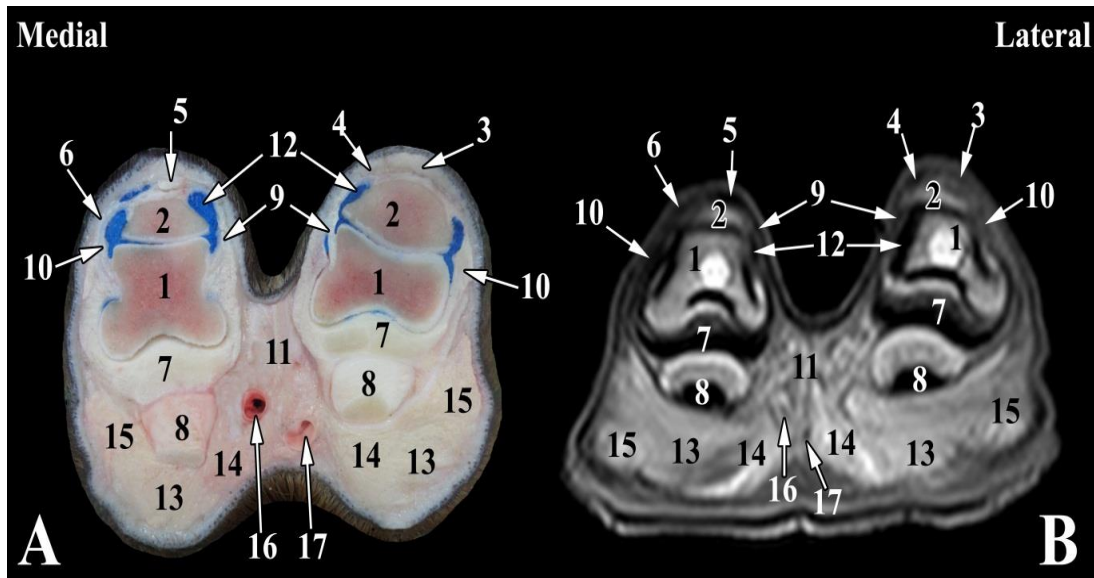


Fig. 4. Transverse images of the right hind distal limb of the dromedary camel at the level of the pastern joint. **A.** Transverse gross anatomical section; **B.** Magnetic resonance image. **1.** Proximal phalanx; **2.** Middle phalanx; **3.** Lateral digital extensor tendon; **4.** Lateral branch of the lateral limb of the common digital extensor tendon; **5.** Medial branch of the lateral limb of the common digital extensor tendon; **6.** Medial limb of the common digital extensor tendon; **7.** Middle scutum; **8.** Deep digital flexor tendon; **9.** Axial collateral ligaments of the pastern joint; **10.** Abaxial collateral ligaments of the pastern joint; **11.** Interdigital ligament; **12.** Joint capsule of the pastern joint; **13.** Middle digital cushion; **14.** Axial digital cushion; **15.** Abaxial digital cushion; **16.** Proper plantar digital artery; **17.** Proper plantar digital vein.

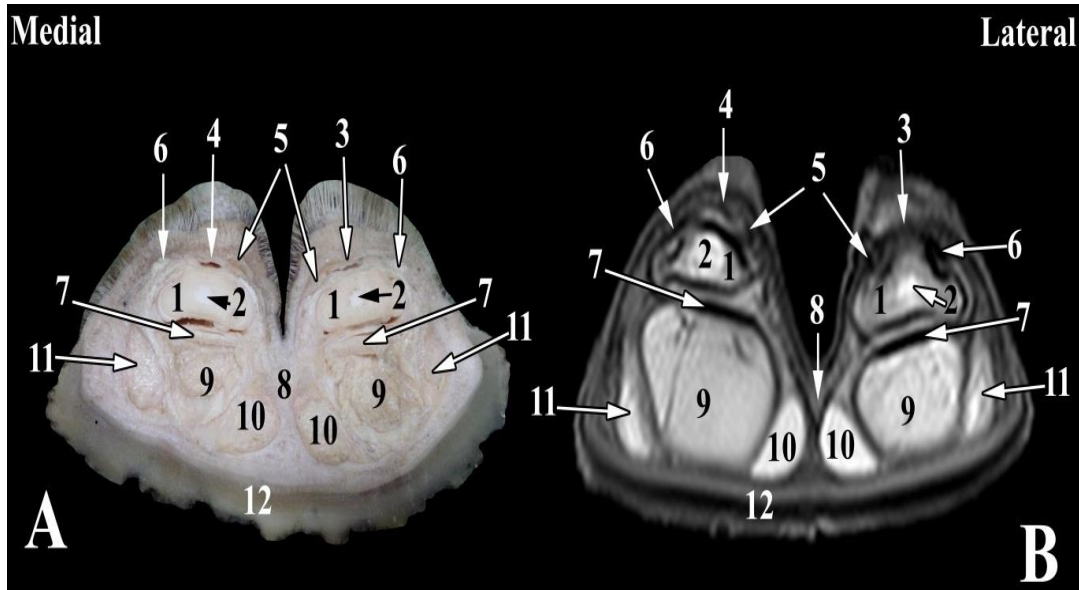


Fig. 5. Transverse images of the right hind distal limb of the dromedary camel at the level of the middle of the second phalanx. **A.** Transverse gross anatomical section; **B.** Magnetic resonance image. **1.** Second phalanx; **2.** Medullary cavity of the second phalanx; **3.** Lateral branch of the lateral limb of the common digital extensor tendon; **4.** Medial branch of the lateral limb of common digital extensor tendon; **5.** Axial dorsal ligaments of the coffin joint; **6.** Abaxial dorsal ligaments of the coffin joint; **7.** Deep digital flexor tendon; **8.** Interdigital ligament; **9.** Middle digital cushion; **10.** Axial digital cushion; **11.** Abaxial digital cushion; **12.** Sole.

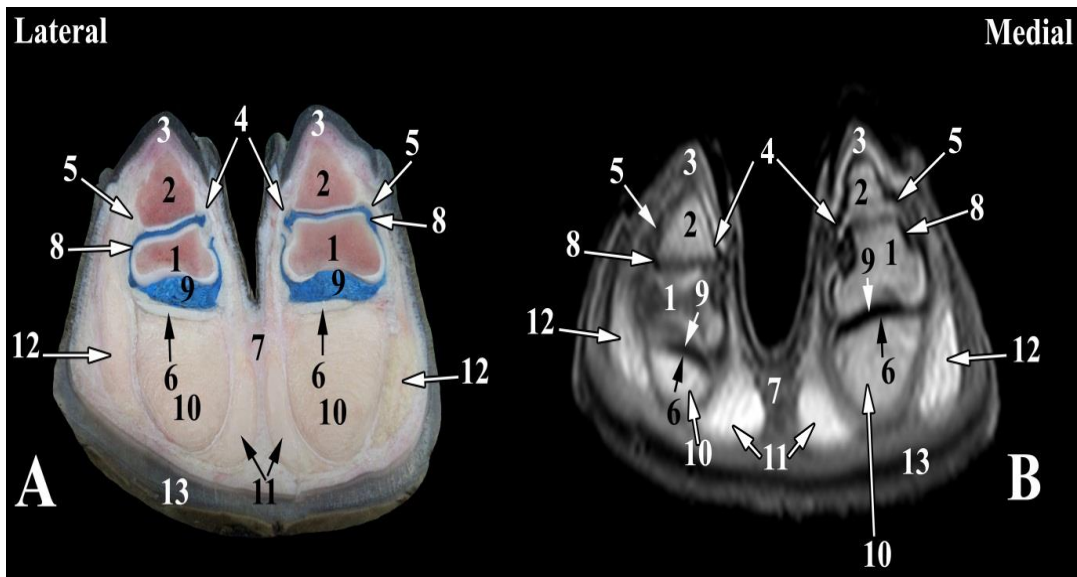


Fig. 6. Transverse images of the left hind distal limb of the dromedary camel at the level of the digital cushion. **A.** Transverse gross anatomical section; **B.** Magnetic resonance image. **1.** Second phalanx; **2.** Third phalanx; **3.** Nails; **4.** Axial collateral ligaments of the coffin joint; **5.** Abaxial collateral ligaments of the coffin joint; **6.** Deep digital flexor tendon; **7.** Interdigital ligament; **8.** Joint capsule of the coffin joint; **9.** Plantar synovial pouch of the coffin joint; **10.** Middle digital cushion; **11.** Axial part of the digital cushion; **12.** Abaxial cushion; **13.** Sole.

4. Discussion

Magnetic resonance imaging is an excellent imaging modality used for scanning of the pastern and coffin joints in dromedary camel. This modality provides visualization of the clinically relevant anatomical structures in three planes and serial slices defining these structures at several angles. Also, using the latex injected joint capsules allowed a precise characterization of the anatomical features of these joints, and provided a standard normal reference for the shape and position of the normal anatomical structures. A T1-weighted MRI was acquired in the current study with minimal slice thickness (2mm) and a high acquisition speed allowing more detailed anatomical structures to be appropriate for practical clinical imaging, similar to the findings obtained by **Smith et al. (2011)**.

Articular cartilages, subchondral bone, cortical bone and cancellous bone were clearly delineated and well-evaluated in the present study. Articular cartilages of second and third phalanges were recognized from the surrounding bony structures as a thin layer of high signal intensity, in matching the findings of **Hagag and Tawfik (2018)** in cattle. On contrary, these cartilages could be observed only using CT in horse (**Vanderperren et al. 2008**). This may be due to the markedly curved articular surfaces of the joints and thin cartilages for the spatial resolution during scanning using the clinical MRI (**Cohen et al. 1999**). Moreover, subchondral bone had a low signal intensity and could be clearly differentiated from articular cartilage at extremities of the second and third phalanges. Also, cancellous bone could be depicted at the extremities of each bone with a high signal intensity, while the cortical bone appeared as a low signal intensity (**Hagag and Tawfik 2018**). The present study reported that the medulla of the second and third phalanges appeared with high signal intensity on the MRI. On the other hand, it appeared as a low signal intensity in cattle (**Raji et al. 2009**) and camel (**El-Shafey and AbdAl-Galil 2012**).

Using MR imaging in this study showed high signal intensities of the middle scutum and navicular cartilage, heterogeneous high signal intensity of the digital cushion, and sole appeared as a layer of low signal intensity between two lines of high signal intensities. However, the nails of camel and hoof of cattle have high signal intensities and appear as black

areas on the MR images (**Raji et al. 2009** in cattle; **El-Shafey and Abd Al-Galil 2012** in camel).

The current study provided a detailed visualization of the ligaments of the pastern and coffin joints using MR imaging. These ligaments included; the collateral ligaments of the pastern joint as well as the interdigital, collateral and dorsal ligaments of the coffin joint, while the palmar/plantar ligaments of the pastern joint and ligaments of the navicular cartilage could not be defined. On the other hand, the ligaments of these joints have not been observed in previous studies of camel distal limbs (**El-Shafey and Abd Al-Galil 2012**; **El-Nahas et al. 2015**).

The extensor and flexor digital tendons were evaluated and clearly outlined in cross anatomical sections and their matched MR images. However, these tendons can be evaluated only in the transverse sections after removal of the intervening fascia in camel distal limbs (**El-Shafey and Abdel AlGalil 2012**). The present study and **Hagag and Tawfik (2018)** in cattle visualized these tendons on the obtained MR images as low signal intensities. The extensor tendons could be visualized as two oval strips on the dorsum of each digit. Moreover, the margins of these tendons were well-outlined by the surrounded fascia that had an intermediate signal intensity, similar to the findings of **El-Nahas et al. (2015)** in camels and **Vanderperren et al. (2008)** in horses. However, these tendons are visualized as narrow undifferentiated strips on the dorsum of each digit on the MR images of camel distal limbs (**El-Shafey and Abd Al-Galil 2012**). Moreover, the present study provided visualization of the extensor tendons on the MR images as a narrow strip distal to the pastern joint which indicated division of the lateral limb of the common digital extensor tendon into two branches; each one ended on the dorsal ridge of the corresponding third phalanx, on contrary to **Smuts and Bezuidenhout (1987)** in camel who reported that the extensor tendons don't reach the third phalanges.

The Joint capsules of the pastern and coffin joints appeared as low signal intensities, while their margins were clearly delineated as thin lines of intermediate signal intensities on all MR images. Similar results were observed in cattle (**Hagag and Tawfik 2018**). However, these capsules could not be detected on the MR images, because they are

considered as potential cavities and appear only in the linear transverse sections in camel distal limbs (El-Shafey and Abd Al-Galil 2012).

5. Conclusion

The current study permitted a definite anatomical description of the compared cross anatomical sections with their corresponding MR images of the clinically relevant structures of the pastern and coffin joints in the dromedary camel. These images could help as a normal reference during the clinical diagnosis of the pastern and coffin joints of such animal species.

6. Conflict of interest

The authors have no conflict of interest to declare

7. References

- Abdellatif AM, Hamed MA, El-Shafaey E, Eldoumani H (2018). Normal magnetic resonance anatomy of the hind foot of Egyptian buffalo (*Bubalus bubalis*): A correlative low-field T1- and T2-weighted MRI and sectional anatomy atlas. *Anat Histol Embryol*. 47: 599-608.
- Ahmad S, Yaqoop M, Hashmi M, Ahmad S, Zaman MA, Tariq M (2010). The economic importance of camel: A unique alternative under crisis. *Park Vet J*. 30(4):191-197.
- Al-Juboori A (2013). Prevalence and etiology of lameness in racing camels (*Camelus dromedarius*) in Abu Dhabi Emirate. *Journal of Camelid Science*, 6: 116–121.
- Arencibia A, Vazquez JM, Rivero M, Latorre R, Sandoval JA, Vilar JM, Ramirez JA (2000). Computed tomography of normal cranioccephalic structures in two horses. *Anat Histol Embryol*. 29: 295–299.
- Cohen ZA, McCarthy DM, Kwak SD, Legrand P, Fogarasi F, Ciaccio EJ, Ateshian GA (1999). Knee cartilage topography, thickness, and contrast areas from MRI: In-vitro calibration and in vivo measurements. *Osteoarthritis and Cartilage*, 7: 95-109.
- El-Nahas A, Hagag U, Brehm W, Ramadan RO, Al Mubarak A, Gerlach K (2015). Computed tomography of the hind limbs in healthy dromedary camel foot. *U. of K. J Vet Med Anim Prod*. 6(2): 98-102.
- El-Shafey AA, Abd Al-Galil ASA (2012). Magnetic resonance image of the one humped (*Camelus dromedarius*) digits. *J American Sci*. 8(9): 549-556.
- Hagag U, Tawfiek MG (2018). Ultrasonography, computed tomography and magnetic resonance imaging of the bovine metacarpo/metatarsophalangeal joint. *The vet J*. 233: 66-75.
- Monfared AL (2013). Applied anatomy of the head regions of the One-humped camel (*Camelus dromedarius*) and its clinical implications during regional anesthesia. *Global Veterinaria*, 10(3): 322-326.
- Nuss K, Schnetzler C, Hagen R, Schwarz A, Kircher P (2011). Clinical application of computed tomography in cattle. *Tierarztl Prax-Ausg G Grosstiere Nutztiere*, 39(5): 317–324.
- Pollard R, Puchalski S (2011). CT contrast media and applications. In: *Veterinary computed tomography*. Schwarz, T. and Saunders J. (eds), Willey-Blackwell, pp. 57- 65.
- Raji AR, Sardari K, Mohammadi HR (2009). Magnetic resonance imaging of the normal bovine digit. *Veterinary Research Communications*, 33: 515-520.
- Sadegh BAM, Shadkhas S, Sharifi A, Mohammadnia HR (2007). Lacrimal apparatus system in one-humped camel of Iran (*Camelus dromedarius*): Anatomical and radiological study. *Iranian J Vet Surgery*, 2(5):76-80.
- Sampson SL, Tucker RL (2007). Magnetic resonance imaging of the proximal metacarpal and metatarsal regions. *Clinical Technical Equine Practice*, 6: 78-85.
- Smith MA, Dyson SJ, Murray RC (2011). The appearance of the equine metacarpophalangeal region on high-field vs standing low-field magnetic resonance imaging. *Vet radiology and Ultrasound*, 52: 61- 70.
- Smuts MMS, Bezuidenhout AJ (1987). *Anatomy of the dromedary*. Oxford, Clarendon Press, pp. 31-90.
- Solano L, Barkema HW, Pajor EA, Mason S, LeBlanc SJ, Zaffino-Heyerhoff JC, Nash CG, Haley DB, Vasseur E, Pellerin D (2015). Prevalence of lameness and associated risk factors in Canadian Holstein-Friesian cows housed in free stall barns. *J Dairy Sci*. 98: 6978–6991.

Vanderperren K, Ghaye B, Hoegaerts M, Saunders JH (2008). Evaluation of Computed Tomographic Anatomy of the Equine Metacarpo-phalangeal Joint. *American J Vet Res.* 69: 631-638.